Long-wavelength vertical-cavity semiconductor optical amplifiers

E. Staffan Björlin

University of California, Santa Barbara; Dept. of Electrical and Computer Engineering

ABSTRACT

Vertical-cavity semiconductor optical amplifiers (VCSOAs) are interesting devices because of their small form factor, potential low manufacturing cost, high coupling efficiency to optical fiber, and polarization independent gain. In this paper, an overview of the properties and possible applications of long-wavelength VCSOAs is given. We present general design rules and analyze how the mirror reflectivity affects the properties of the VCSOA. Experimental results of reflection-mode VCSOAs operating at 1.3-µm wavelength are presented. The devices were fabricated using InP-GaAs wafer bonding and were optically pumped by a 980-nm laser diode. These VCSOAs have demonstrated the highest fiber-to-fiber gain (17 dB), as well as the highest saturation output power (-3.5 dBm) of any long-wavelength VCSOA to date. We have also used these VCSOAs for optical preamplification at 10 Gb/s. Using an 11-dB gain VCSOA, the sensitivity of a regular *PIN* detector was increased by 7 dB resulting in a receiver sensitivity of –26.2 dBm.

Keywords: Semiconductor optical amplifiers, laser amplifiers, vertical-cavity devices, Fabry-Perot resonators.

1. BACKGROUND

There is currently significant interest in amplifier technologies that can provide a cost-effective alternative to the ubiquitous erbium doped fiber amplifier (EDFA). Potential low-cost technologies such as erbium doped waveguide amplifiers (EDWAs) and semiconductor optical amplifiers (SOAs) are being pursued by several companies. An alternative to the conventional in-plane SOAs are vertical-cavity semiconductor optical amplifiers (VCSOAs). The vertical-cavity design gives VCSOAs a number of advantages over in-plane devices, such as high coupling efficiency to optical fiber, small form factor, low power consumption, and the possibility of fabricating two-dimensional arrays on wafer. Furthermore, the technology allows for on-wafer testing and is compatible with low-cost manufacturing and packaging techniques. These advantages all draw from the fundamental geometrical differences between the vertical-cavity and the in-plane designs. In a vertical-cavity structure the optical mode passes perpendicularly through the different material layers. Consequently, the optical field is always parallel to the active layers, which makes it easier to obtain polarization independent gain. It also makes the gain per pass very small, on the order of a few percent. VCSOAs therefore use feedback provided by high reflectivity distributed Bragg reflector (DBR) mirrors. The feedback constricts the gain bandwidth to the linewidth of the Fabry-Perot mode, which essentially limits the operation to amplification of a single signal. The narrow bandwidth also filters out out-of-band noise, making VCSOAs ideal as preamplifiers in receiver modules. The vertical cavity is circular symmetric around the axis perpendicular to the two mirrors and naturally supports a circular optical mode. This yields high coupling efficiency to optical fiber, which is beneficial for achieving a low noise figure.

VCSOAs are a relatively unexplored technology but a handful of devices have been presented throughout the past decade. The first VCSOA was demonstrated in 1991 by Koyama, Kubota, and Iga at Tokyo Institute of Technology. They used an electrically pumped GaAs/AlGaAs VCSEL structure to amplify and filter an injected 885-nm signal[1]. The device had a bulk active region and a combination of SiO_2/TiO_2 and gold mirrors. No fiber-to-fiber gain was obtained but about 4 dB internal gain was reported. Two years later, in 1993, an optically pumped 850-nm VCSOA was presented by Raj *et al.* at France Telecom. Only pulsed operation was reported[2]. The same group introduced resonant

pumping in a following generation of 850-nm devices[3] and in 1996 they presented the first long-wavelength VCSOA[4]. The sample consisted of an InP/InGaAs active region with two sets of 5 quantum wells, a gold bottom mirror and a two period Si-SiO$_2$ top mirror. It was optically pumped and operated in reflection mode. The operating wavelength was 1.55 µm. 14 dB of gain was achieved in pulsed operation. Also in 1996, Wiedenmann *et al.* at University of Ulm presented an electrically pumped reflection mode VCSOA operating at 980 nm[5]. Two years later, in 1998, they modified the design and incorporated an oxide aperture for current and mode confinement. They achieved 16 dB of gain[6]. In 1998, Lewen *et al.* at KTH in Sweden used a 1.55 µm VCSEL structure for what was the first electrically pumped long wavelength VCSOA[7]. The device had an InP/InGaAsP bottom DBR and a Si/SiO$_2$ top DBR. They measured 18 dB of gain at 218 K not including coupling losses (fiber-to-fiber gain was not quoted). The VCSOA project at UCSB started in 1999 and lead to the demonstration of the first 1.3-µm VCSOA in 2000[8]. These devices were fabricated using InP-GaAs wafer bonding, they were optically pumped, and operated in reflection mode. This first generation was used to fully characterize this still fairly new class of devices[9,10], to develop improved theoretical models[11,12], and to explore possible applications for VCSOAs[13,14]. A second generation of 1.3-µm devices with improved efficiency and record-high gain was recently presented[15]. The VCSOA-project at UCSB has recently been expanded to include electrically pumped long-wavelength devices[16].

In this paper we overview of the properties and possible applications of long wavelength VCSOAs. In Section 2, general VCSOA theory is presented and a few useful design rules are derived. The effect that the reflectivity of the mirrors has on the VCSOA properties is analyzed. In Section 3, results of two generations optically pumped 1.3-µm VCSOAs fabricated at UCSB are presented. A few potential applications for these VCOSAs are discussed in Section 4, including optical interconnects, switching and modulation, and optical preamplification for high bit-rate receivers.

2. VCSOA DESIGN

VCSOAs are in principle VCSELs operated below lasing threshold. Materials and processing technologies developed for VCSELs can be directly applied to VCSOAs, and the design of the two is in many ways similar. The different VCSOAs presented over the past decade have shown great diversity in design and materials. Some have been optimized as amplifiers; some were merely VCSELs operated below threshold. Some structures were all-epitaxial, some used deposited insulating DBRs, and some used wafer bonding to combine long-wavelength InP-based active regions with high reflectivity AlGaAs DBRs. Almost all of the presented devices rely on multiple quantum well active regions to provide the high single-pass gain needed to reach sufficient amplifier gain. Only one device, the first VCSOA[1], used a bulk active region. Several designs include a longer cavity with two or more stacked MQW active regions that provide periodic gain that matches the standing wave pattern in the cavity. This stacked MQW active region design is very attractive for VCSOAs since they require significantly higher single-pass gain than VCSELs. The long wavelength devices presented so far have all used InGaAsP based QWs[4,7]. In long-wavelength VCSELs, significant progress has been made recently using AlInGaAs QWs for 1.55 µm emission[17], GaInNAs grown on GaAs for 1.3 µm[18], and Sb-based structrures[19]. AlInGaAs provide improved high temperature performance due to its larger conduction band offset and GaInNAs has the advantage of being lattice matched to GaAs. No VCSOAs have yet been reported using these materials.

The typically large number of QWs needed to achieve high gain makes it difficult to pump the QWs uniformly using electrical injection. Optical pumping is an attractive way to pump VCSOAs for a number of reasons. Optical pumping generates carriers in the QWs, without the need of transporting the carrier through the structure. This results in very uniform carrier distribution throughout a large number of QWs. It also allows the entire structure to be undoped, which simplifies growth and processing, and minimizes optical losses. Furthermore, optical pumping can generate uniform carrier distribution across a laterally large active region. Optical pumping is not just a tool for the lab. Device and pump laser can be packaged in the same package, or even integrated into the same structure[20]. Several high-performance long wavelength VCSELs have been presented that use optical pumping[20,21] and these devices have recently been taken into manufacturing[22].

VCSOAs can be operated in two different configurations: reflection mode or transmission mode operation, as depicted in Figure 1. In reflection mode devices, the signal enters the cavity from the top, through the top DBR, and comes back out the same way. A bottom mirror reflectivity close to unity is desired, and the top mirror reflectivity can be varied to change the properties of the devices. It is easier to achieve good amplifier characteristics in this configuration. It might also be a more cost effective approach since the fiber alignment, which is a very difficult and costly step in the manufacturing, is reduced from two fibers to one. However, the input and output signals need to be separated. The separation calls for an additional component (coupler or circulator), which adds complexity, cost, and signal loss. Operation in transmission mode is more attractive in some applications, *e.g.* integration with detectors for pre-amplification or array applications. It is, however, a more difficult approach as far as testing and packaging. The choice of operational mode might ultimately depend on the intended application for the VCSOA.
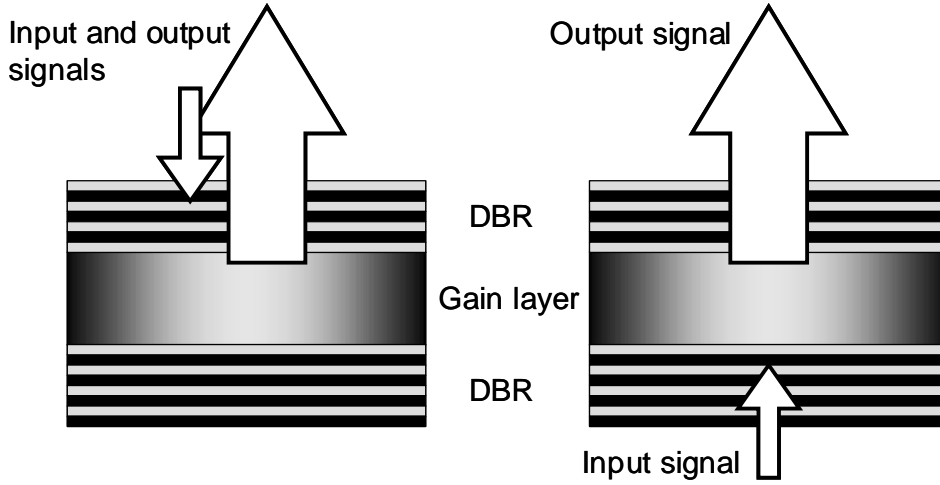

Figure 1. Schematic of VCSOAs showing reflection mode operation (left) and transmission mode operation (right).

Central to the design of VCSOAs is the balance between the gain provided by the active region and the reflectivity of the two mirrors. Strong feedback, *i.e.* high reflectivity, naturally results in high amplifier gain for a given value of single-pass gain. However, if the net gain per roundtrip equals unity the device starts to lase. The amplifier gain is in the high reflectivity regime limited by lasing threshold. If the reflectivity is too low, there will not bee enough feedback to reach sufficient amplifier gain, and the amplifier gain is in this case limited by the material gain provided by the active region. The reflectivity should be just low enough so that lasing threshold is not reached when the amplifier is driven at full population inversion, *i.e.* the available material gain should be fully utilized.

To model the gain spectrum of VCSOAs, the well-known Fabry-Perot equations for an active filter can be used[23]. These equations are a convenient tool to model basic VCSOA trends, and to understand the behavior of these devices. In this model the DBRs are replaced by hard mirrors separated by an effective cavity length, which includes the penetration of the optical field into the mirrors. An incoming optical field is considered and all field components exiting the cavity are added together to get the output field. To obtain the power gain, the fields are squared and the total output power is divided by the input power. The gain for reflection mode (G_r) and transmission mode (G_t) operation are given by

$$G_r = \frac{(\sqrt{R_t} - \sqrt{R_b}\, g_s)^2 + 4\sqrt{R_t R_b}\, g_s \sin^2 \phi}{(1 - \sqrt{R_t R_b}\, g_s)^2 + 4\sqrt{R_t R_b}\, g_s \sin^2 \phi} \tag{1}$$

$$G_t = \frac{(1 - R_t)(1 - R_b)\, g_s}{(1 - \sqrt{R_t R_b}\, g_s)^2 + 4\sqrt{R_t R_b}\, g_s \sin^2 \phi} \tag{2}$$

where R_t is the top mirror reflectivity, R_b is the bottom mirror reflectivity, g_s is the single pass gain, and ϕ is the round-trip phase detuning normalized to the cavity resonance. Note that the gain of a transmission mode device is independent of the direction of signal propagation through the device. If ϕ is set equal to zero, Equations 1 and 2 can be used to calculate the peak gain. From these equations, formulas for calculating the bandwidth are readily obtained. The gain bandwidth (FWHM) for the two cases are given by

$$\Delta f_r = \frac{c}{\pi n L} \cdot \arcsin\left[4\sqrt{R_t R_b}\, g_s \left(\frac{1}{(1-\sqrt{R_t R_b}\, g_s)^2} - \frac{2}{(\sqrt{R_t}-\sqrt{R_b})^2} \right) \right]^{-\frac{1}{2}} \tag{3}$$

$$\Delta f_t = \frac{c}{\pi n L} \cdot \arcsin\left[\frac{(1-\sqrt{R_t R_b}\, g_s)^2}{4\sqrt{R_t R_b}\, g_s} \right]^{\frac{1}{2}} \tag{4}$$

where n is the refractive index of the cavity, L is the effective cavity length, and c is the velocity of light in vacuum. Figure 2 shows calculated peak gain and gain bandwidth as a function of mirror reflectivity for different values of single-pass gain (1% - 5% for reflection mode, 2% - 5% for transmission mode). The graph to the left shows reflection mode operation, the graph to the right shows transmission mode operation. The cavity length used in these calculations is 2.2 μm, which is the cavity length of the devices presented later in this paper. A longer cavity yields a narrower bandwidth. For the case of reflection mode operation, a bottom mirror reflectivity of 99.9% is used in the calculations and gain and bandwidth are plotted versus top mirror reflectivity. The bandwidth of reflection mode devices approaches infinity for low peak gain since there is a constant wavelength independent reflection off the top mirror. For the case of transmission mode operation, the reflectivity of one mirror is held constant at 95% while the reflectivity of the other mirror is varied. The dashed lines indicate lasing threshold. Operation too close to lasing threshold must be avoided and the high gain values suggested by the steep part of the curves are difficult to achieve in practice. The single pass gain needed to achieve high amplifier gain is higher for the case of transmission mode operation because of the higher combined mirror loss. These graphs give the impression of a trade-off between gain and bandwidth. However, this is only true for a constant single-pass gain. In the regime where the VCSOA can be brought to lasing threshold, low reflectivity allows for stronger pumping and thereby higher gain. It can be shown that the gain-bandwidth product increases with decreased mirror reflectivity[24].
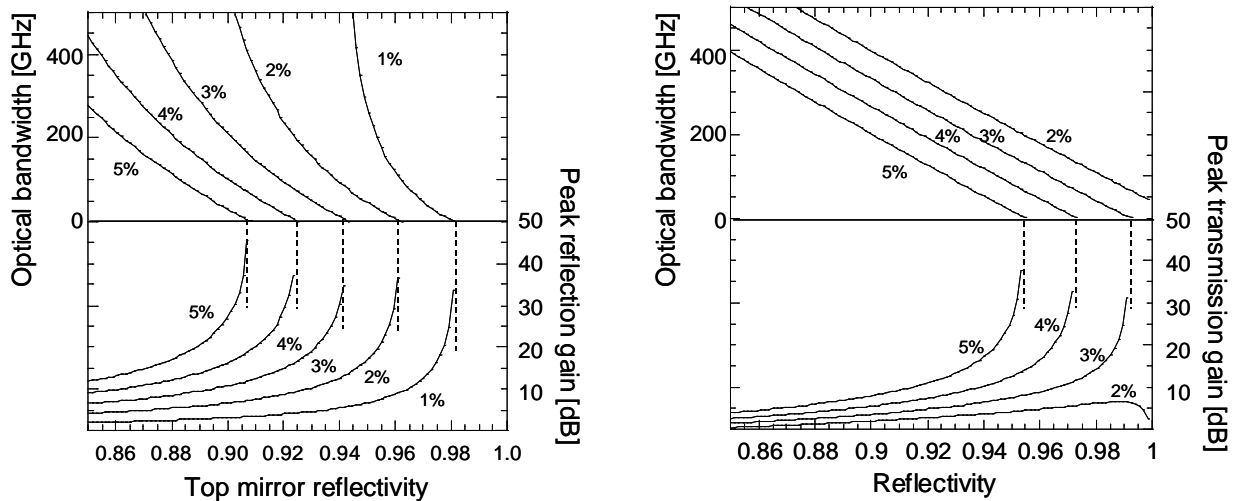

Figure 2. Gain and gain bandwidth for VCSOAs operated in reflection mode (left) and transmission mode (right). The curves represent different values of single-pass gain, as indicated in the figure.

The noise figure of an optical amplifier describes the signal to noise ratio (SNR) degradation as a signal passes through the amplifier. This makes the noise figure one of the most important properties of optical amplifiers for their applications in optical communication systems. The noise figure of VCSOAs can be analyzed using the same methods as for in-plane Fabry-Perot amplifiers[25]. The total output noise from an optical amplifier consists of several different noise terms of different origin. The terms contributing to the total noise are: beating between amplified spontaneous emission (ASE) components and the coherent signal light, beating between different ASE components, and shot noise due to both signal and ASE. The input signal might also have some excess noise and the receiver adds thermal noise. Spontaneous-spontaneous beat noise is independent of the input signal power and is the dominating term at low signal power. This term depends on the optical bandwidth of the ASE spectrum. For this reason, a bandpass filter is normally used after the optical amplifier in order to minimize the amount of ASE reaching the detector. This is not needed for a VCSOA as the spontaneous emission bandwidth is limited by the Fabry-Perot cavity. Signal-spontaneous beat noise and shot noise increase with input signal power. At high signal powers signal-spontaneous beat noise is the main contributor to the output noise. The output ASE, and hence the signal-spontaneous beat noise is greatly affected by the mirror reflectivity.

Considering signal-spontaneous beat noise to be dominant, the noise factor, F, defined as input SNR over output SNR (the noise *figure* is defined as $NF=10\log(F)$ and expressed in decibels), is given by $F=2n_{sp}\chi(G-1)/G$, which for high signal gain ($G \gg 1$) reduces to $F=2n_{sp}\chi$. Here, n_{sp} is the population inversion parameter and χ is the excess noise coefficient, which describes signal-spontaneous beat noise enhancement due to finite mirror reflectivity. χ takes a value of one for zero reflectivity (the case of traveling wave amplifiers) and values higher than one for finite mirror reflectivities. An excess coefficient of one can be obtained for VCSOAs if the mirror reflectivities are chosen properly[10]. For a reflection mode device, χ depends only on the bottom mirror reflectivity, which should be as high as possible. For a bottom mirror reflectivity over 99.9%, which is easily obtained using DBR mirrors, χ equals one. For the case of transmission mode operation, low input mirror reflectivity is desired in order to minimize χ. The population inversion parameter n_{sp} equals one for complete inversion and higher values for incomplete inversion. It is desired to operate at as high carrier density as possible in order to minimize n_{sp}. A problem inherent to FP-amplifiers is that the strong pumping needed to minimize n_{sp} could result in lasing if the mirror reflectivity is to high. It is therefore of utmost importance that the mirror reflectivities are low enough to allow full inversion without the onset of lasing. For any practical application, the often critical parameter is not the intrinsic noise figure of a device but rather its fiber-to-fiber noise figure. The noise figure is degraded by loss associated with coupling of the signal into the VCSOA (in logarithmic units, the input coupling loss is simply added to the noise figure). VCSOAs have superior coupling efficiency compared to in-plane devices and can therefore be expected to show better fiber-to-fiber noise figures, close to the fundamental limit of 3 dB.

As the photon density in the cavity is increased, the gain medium eventually saturates and the gain drops. This occurs when the signal power is increased or when the VCSOA is operated close to threshold in which case the ASE causes gain saturation. The saturation properties of the VCSOA can be modeled using rate equations that describe the balance between carriers and photons in the cavity[11]. Compared to the well-known rate equations commonly used to analyze lasers, these have an additional term for the input signal. Furthermore, the mirror loss has to be modified to include interference as there are optical fields traversing one of the mirrors (on the input side) in both directions[12]. For high saturation power (and high output power) it is clearly desirable to maintain a large carrier density to photon density ratio as the signal power is increased. This can be achieved by making the active volume large and reduce the photon cavity lifetime (lower photon density) and pump the device hard (high carrier density). The drawback is that high gain in a large active volume leads to higher power consumption. The mirror reflectivity is important also for the saturation properties since it affects the photon cavity lifetime.

To summarize the theory trends, strong feedback, *i.e.* high mirror reflectivity, leads to high gain for a given value of single pass gain, but the gain is limited by lasing threshold. It also leads to poor noise figure and early saturation. For optimum performance, it is desirable to use mirror reflectivities that are high enough to yield high signal gain, but low enough to allow operation at high carrier density without lasing to occur. This condition gives the highest possible amplifier gain and gain -bandwidth product, the highest saturated output power and the lowest noise figure.

3. EXPERIMENTAL AMPLIFIER RESULTS

Two generations of VCSOAs have been developed at UCSB. Both generations operated at 1.3-μm signal wavelength and were optically pumped by a 980-nm laser. Both generations comprised a stacked InP/InGaAsP active region wafer bonded to two GaAs/Al$_{0.9}$Ga$_{0.1}$As DBRs. Figure 3 shows the refractive index profile and the standing wave in the 5/2-λ cavity. The active region had three sets of seven compressively strained InAs$_{0.5}$P$_{0.5}$ quantum wells surrounded by strain compensating In$_{0.8}$Ga$_{0.2}$P barriers. The three sets of QWs were positioned on the three central standing wave peaks in the cavity to maximize the optical mode-QW overlap. The wafer bonded interfaces were placed at nulls in the optical field in order to minimize scattering losses at the interfaces. Details about wafer bonding are reported elsewhere[26]. Both generations of devices were designed for reflection mode operation; the bottom DBR had 26 periods, giving a calculated reflectivity of 99.9%. They were made from the same active region material to facilitate a quantitative comparison of the two designs. Generation 1 was a gain guided, planar structure where the lateral dimensions of the active region were defined by the spot size of the pump laser beam. The number of top mirror periods was varied in the characterization of the device by selectively etching off individual mirror periods. The results from these devices were in good agreement with theoretical predictions. High gain (13.5 dB, fiber to fiber) and high saturated output power (-3.5 dBm) was obtained. However, the efficiency of these devices was low as a substantial fraction of the carriers were lost due to lateral diffusion in the QWs, out of the active region. Generation two had etched mesas in the active region to provide carrier confinement. This simple design improvement turned out to have a significant impact on the efficiency and maximum amplifier gain, as compared to Generation 1.
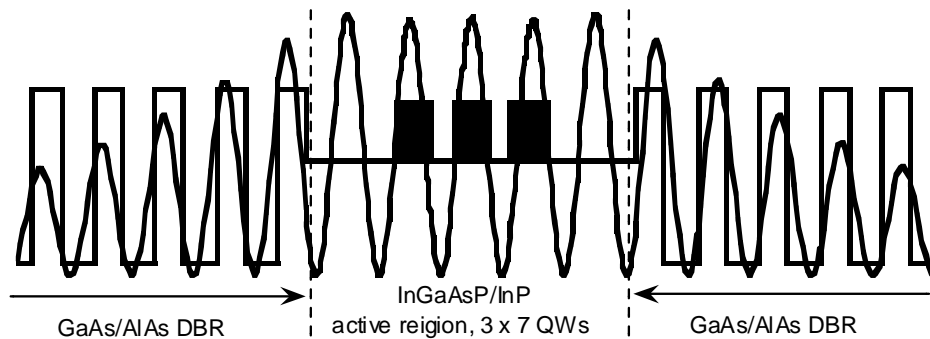

InGaAsP/InP
active reigion, 3 x 7 QWs

GaAs/AlAs DBR   GaAs/AlAs DBR

Figure 3. Refractive index profile and standing wave distribution in 5/2-λ cavity of wafer bonded VCSOA. Quantum wells are positioned on peaks; bonded interfaces at nulls (indicated by dashed lines).

A 980-nm laser diode was used to pump the VCSOAs through the substrate and bottom DBR. The pump beam was focused down on the VCSOA active region using free-space optics, to a spot size of 8 μm. A 1.3-μm external cavity tunable laser diode was used as signal source. A single-mode fiber and a lens were used to inject the 1.3-μm signal through the top mirror of the device and to collect the output signal. The spot size of the signal was about 7.5 μm. The input and the output signals were separated by means of an optical circulator. The total coupling loss (including loss in the circulator) was about 7 dB. An optical spectrum analyzer was used to monitor the output signal.

Figure 4 shows optical bandwidth versus fiber-to-fiber gain for two VCSOAs from Generation 1. The reflectivities of the devices were 96% and 96.5%. The input signal power was -25 dBm. The dots are measurements and the lines are curve fits based on Equations 1 and 2. Good agreement between measured data and theory is demonstrated. The curve fits suggest that very high gain and very narrow bandwidth is possible. In practice however, this is limited by lasing threshold. The highest gain measured for Generation 1 was 13.5 dB, fiber-to-fiber, for devices with a top mirror reflectivity of about 95%. For further reduced top mirror reflectivity the devices could not be brought to lasing threshold and the gain was limited by maximum material gain. Gain bandwidths between 20 – 100 GHz ware measured for Generation 1. The widest bandwidth of 100 GHz was measured for a top mirror reflectivity of 91% and a peak gain of 11 dB.
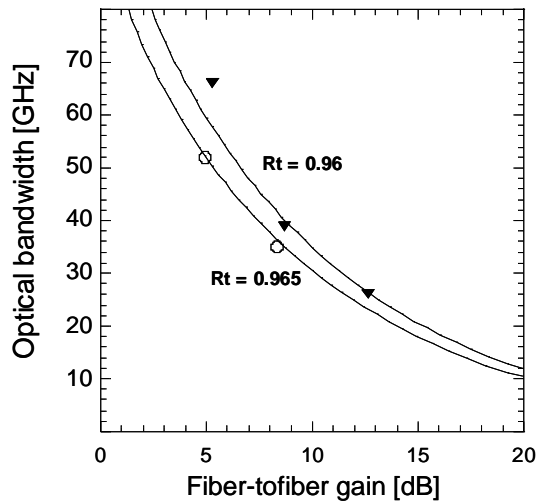
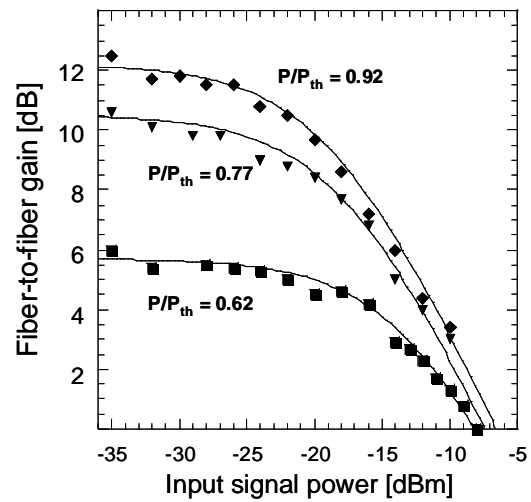Figure 4. Optical bandwidth versus gain for top mirror reflectivities of 96% and 96.5%.

Figure 5. Saturation behavior of a Generation-1 VCSOA with 96% top mirror the reflectivity.

Figure 5 shows gain versus input signal power for a Generation-1 VCSOA. The top mirror reflectivity of this device was 96%. The dots are measurements and the lines are curve fits based on the relation $G = G_0/(1+P/P_{sat})$. The three sets of data represent pump levels relative to lasing threshold of $P/P_{th} = 0.62$, 0.77, and 0.92 ($P_{th} = 130$ mW). It is evident from the graph that as the device was pumped closer to threshold it saturated earlier (lower input saturation power). The *output* saturation power was constant about –9.5 dBm as the pump level was increased. The best saturation output power of Generation 1 was –3.5 dBm, measured for a small signal gain of 11 dBm, and a pump power of 120 mW. The top mirror reflectivity of that devices was 91%. The conclusion from Generation 1 was that the optimum top mirror reflectivity for that active region design was lower than 95%, but not as low as 91%. Unfortunately, no data was taken for reflectivities between 95% and 91% due to an unsuccessful mirror etch. This optimum reflectivity did not agree with the maximum single-pass gain that the active region was designed to be able to provide; much better performance at reflectivities lower than 91% was predicted by theory. Apparently the carrier losses imposed a limit on the maximum achievable carrier density and hence on the maximum gain.

In the fabrication of the second generation of devices circular mesas were etched in the active region prior to bonding the top DBR to the active region. The QWs were also under-etched to create a step-like sidewall profile with the InP cladding layers being slightly larger than the active region. This minimized the length of the semiconductor-air interface compared to mesas without under-etched QWs. Consequently, it reduced scattering loss and provided for weaker index-guiding, which is advantageous for operation in the fundamental TEM_{00} mode. Unfortunately, the under-etch created slightly non-circular active regions, which resulted in a small polarization dependent gain. However, this can easily be avoided through optimized processing. The under-etch allowed InP to migrate through mass-transport from the cladding layers to the sidewalls of the QWs, thereby decreasing the surface recombination and further improve the carrier confinement. Based on the results from Generation 1, the top mirror reflectivity was designed to be about 92% in order to allow for strong pumping and thus high amplifier gain, high saturation power and low noise figure. The top DBR that was used had 10.5-periods, which gives a calculated reflectivity of 91.8%. It turned out that very high single-pass gain could be reached because of the carrier confinement, and optimum performance would have required even further reduced reflectivity.

Fiber-to-fiber gain versus pump power for a VCSOA with a 9-μm active region is shown in Figure 6. The input signal power is –30 dBm. 10 dB of fiber-to-fiber gain was measured for a pump power of 33 mW. The maximum fiber-to-fiber gain was 17 dB, which, considering a total coupling loss of about 7 dB, means that the intrinsic gain was about 24 dB. This is the highest reported gain for any long wavelength VCSOA to date. The efficiency as indicated by the dashed line was 0.34 dB/mW. The gain bandwidth for a peak gain of 15 dB was measured to be 32 GHz, the saturation output power was –5 dBm, and the fiber-to-fiber noise figure was 6.1 dB.
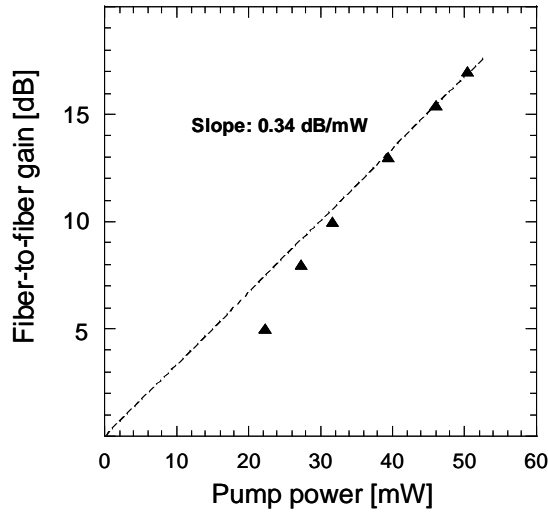
Figure 6. Gain versus pump power for a carrier confined VCOSA with 9 μm diameter active region and –30 dBm input signal power. The efficiency was 0.34 dB/mW (dashed line).
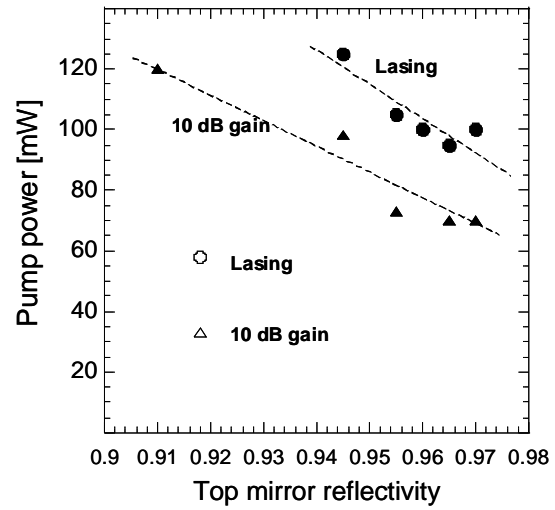
Figure 7. Comparison of planar devices (solid dots) and laterally carrier confined devices (open markers). The graph shows pump power needed to reach 10 dB gain and lasing threshold.

Figure 7 compares the performance of the two generations of VCSOAs. The pump power required to reach 10 dB of fiber-to-fiber gain and lasing threshold is plotted versus top mirror reflectivity. For Generation 1, the lowest required pump power needed for 10 dB gain was about 70 mW, for the high reflectivity devices. The linear curve fit can be used to find the needed pump power at a reflectivity of 91.8%, which was the top mirror reflectivity of Generation 2. At that reflectivity, the planar design would need about 110 mW of pump power to give 10 dB gain, whereas the carrier confined design only needed 33 mW. This corresponds to a 3-fold improvement in efficiency. The planar design could not be brought to lasing threshold at that reflectivity. The 9-μm device from Generation 2 lased at 60 mW of pump power. The fact that lasing threshold can be reached suggests that the QW gain is now high enough so that the reflectivity could be even further reduced. This would result in higher saturation power, lower noise figure, and probably even higher amplifier gain.

4. APPLICATIONS

VCSOAs have a number of potential applications in optical communication systems. Compared to other amplifier technologies the VCSOA bandwidth is very narrow and the saturation power relatively low. The noise figure of VCSOAs can be much lower than for in-plane SOAs. The performance cannot match that of erbium doped fiber amplifiers but the unique characteristics of VCSOAs make them ideal for certain applications. The most obvious features of VCSOAs are the potential low manufacturing cost, their potential for array applications, and the narrow bandwidth, which hinders amplification of multiple channels but provides filtering and channel selection. Proposed applications include optical interconnects, switching/modulation, and optical pre-amplification of high speed receivers.

Free-space optical interconnections are the most promising way to solve the wiring bottleneck between silicon chips in computers[27,28]. The transmitters in these interconnections can be either VCSEL arrays or modulators with an external laser source. The attributes of VCSOAs that make them attractive for use in optical interconnects are their circular beam profile, low power consumption and compatibility with 2D array architectures. Proposed applications are as modulators, preamplifiers, or buses. As modulators, they are an alternative to MQW electro-optic modulators. Better extinction ratio and low voltage operation are here foreseen advantages[29]. An array of preamplifiers integrated with a receiver array would ease the requirements on both transmitters and receivers. This would lead to decreased power dissipation, which in turn would enable higher interconnect density[30]. The optical bus, or repeater, can serve as detector and amplifier in

interconnects between multiple board. Part of the signal is detected and part is passed through to the next board. The amplifier compensates for coupling loss and power absorbed by the detector[31].

Using SOAs for routing of signals is attractive because of their fast gain dynamics, typically large extinction ratio, and the fact that amplifier gain compensates coupling losses. The gain dynamics enable sub-nanosecond switching-time, which is needed in future all-optical packet switched systems. The use of in-plane SOAs for switching has been extensively studied[32-34]. Limiting factors for in-plane SOAs are polarization dependence and accumulation of amplified spontaneous emission (ASE) as switches are cascaded into switch matrices[34]. The accumulation of ASE can be mitigated by the filtering effect of the narrow VCSOA bandwidth. No multiport switches based on VCSOAs have yet been demonstrated but the switching properties of individual VCSOA elements have been studied. A vertical-cavity amplifying switch operated in reflection mode at 1.55-μm wavelength has demonstrated a switching time of 10 ps and an extinction ratio of 14 dB[4]. At 1.3 μm, a reflection mode VCSOAs demonstrated similar switching times and 35 dB extinction ratio[13]. The switching properties of transmission mode VCSOAs have not yet been investigated.

As mentioned above, VCSOA-modulators have been proposed for use in optical interconnects. Amplifying modulators are also attractive for a number of other applications. For example, the gain could compensate for losses associated with division of a signal for transmission to multiple recipients. Another application is the use of SOAs as remote modulators in networks with a centralized light source. Several proposed solutions for access and fiber to the home (FTTH) networks take this approach, instead of using conventional transceivers, in order to minimize component cost[35-37]. The potential low manufacturing cost of VCSOAs would be a major advantage for these applications. In the configuration in Ref[36] SOAs are used both to detect the incoming signal at the remote nodes and to modulate a continuous wave (CW) signal for the upstream information. A VCSOA showing amplifier-detector dual functionality has already been demonstrated[7]. There have been several reports on VCSOA-modulators[29,38]. Small signal modulation at 2.5 Gb/s with 5.5 dB fiber-to-fiber gain was demonstrated in Ref[38].

Using VCSOAs for optical preamplification might be one of the most interesting applications for these devices. At higher bit rates (10 Gb/s, 40 Gb/s, and beyond) avalanche photo diodes are limited by their gain-bandwidth product. Optical preamplification is a way to increase the sensitivity of a regular *PIN*-detector without compromising its high-speed performance. Optical preamplification has been demonstrated using other amplifier technologies (in-plane SOAs, EDFAs) but VCSOAs have some clear advantages. Desired properties for this application are good noise performance and polarization independent gain, which are areas of difficulty for in-plane devices. Also desired are low power consumption, compactness, and low cost, properties that are not associated with fiber amplifiers. VCSOAs can meet all these criteria. Furthermore, an optical filter is normally added after the amplifier for this application, something not needed if VCSOAs are used as their narrow bandwidth makes them function as amplifying filters. The low saturation power of VCSOAs is not a problem for optical preamplification as the signal power reaching the receiver is typically optimized at a lower level than the saturation power of a VCSOA.

We have investigated the feasibility of using our reflection mode VCSOAs for optical preamplification at 10 GB/s[14]. We used a similar setup to the one used for basic VCSOA characterization described above. The input signal was modulated using a 10-Gb/s pattern generator driving a LiNbO$_3$ Mach-Zehnder modulator. The optically preamplified receiver consisted of the VCSOA, a Nortel PP-10G *PIN* receiver, a DC block, and an SHF broadband amplifier. The electrical signal from the SHF amplifier was fed to a bit error rate tester. No optical filter was used between the VCSOA and the *PIN* detector. The receiver sensitivity was measured with and without the VCSOA preamplifier. A 10 Gb/s non-return-to-zero 2^{31}-1 pseudo-random bit sequence was transmitted to the receiver and the bit error rate (BER) was measured. The BER versus average received optical power is shown in Figure 8. Without the VCSOA, the receiver sensitivity corresponding to a BER of 10^{-9} was –19.2 dBm. With the VCSOA operating at 11 dB fiber-to-fiber gain, the receiver sensitivity was improved by 7 dB, resulting in a sensitivity of –26.2 dBm. No error floor was observed. The eye pattern at a BER of 10^{-9} is also shown in Figure 8. Excess noise from the optical amplification is visible in the high level. The 4-dB power penalty is caused by the high noise figure of the VCSOA used in the experiment. The device was one of the Generation-1 devices described above with a top mirror reflectivity of 95.5%. At that reflectivity, the population inversion that could be reached was limited by lasing threshold. This resulted in a noise figure higher than 10 dB. The VCSOAs of the second generation has not yet been used for any transmission experiments, but the receiver sensitivity (for the same *PIN* detector) can be calculated from the measured gain and noise figure of those devices.

Using the best results of Generation 2, fiber-to-fiber gain of 17 dB and a noise figure of 6.1 dB, a receiver sensitivity of − 31.3 dBm is calculated.

These examples are just a few of the possible applications for VCSOAs; many more will certainly arise in the future. It is interesting to note that in most of the VCSOAs publications to date the multifunctionality of these devices have been stressed. The devices have been presented as amplifying filter[1], amplifying switch[2-4,13], amplifying detector[7], etc. One potential path for VCSOAs is towards integration with other devices, *e.g.* VCSELs, detectors, etc. The vertical access and array compatibility are here clear advantages. The most important step for VCSOAs is probably to make these devices tunable to cover a wider wavelength range. The wavelength requirements on sources in low-cost course WDM systems is fairly loose, which has to be accommodated by the amplifiers in the system. Tunable VCSOAs could be realized by employing micro electromechanical systems (MEMS), similar to what is being used for tunable VCSELs[21,22]. One example of an interesting possibility for a future device is shown in Figure 9. It is a tunable VCSOA integrated with a photodetector. This device takes full advantage of the filtering properties of VCSOAs and would be very attractive as a tunable, wavelength selective receiver for application in WDM systems. This could be either single devices or 2D arrays for parallel applications.
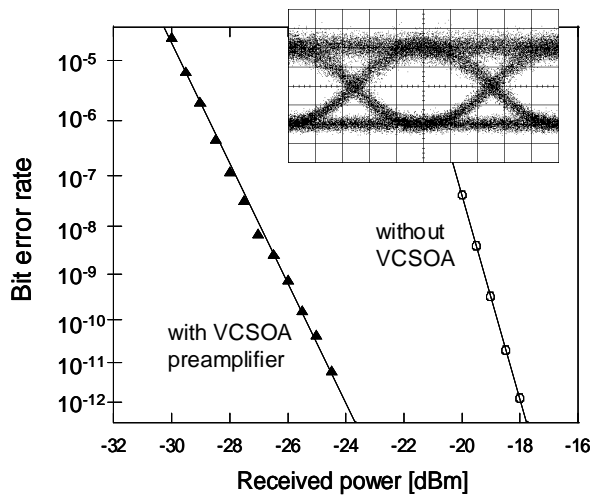

Figure 8. BER at 10 Gb/s, with and without VCSOA pre-amplification. Inset shows eye pattern at BER = 10^{-9} with the VCSOA.
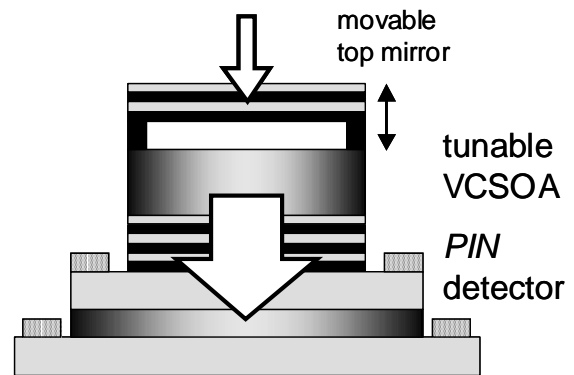
Figure 9. Tunable wavelength selective receiver comprising a tunable VCSOA integrated with a *PIN* photodetector.

5. SUMMARY

VCSOAs are a relatively new class of devices with unique properties. Compared to conventional in-plane SOAs they have much lower gain per pass and therefore use feedback provided by mirrors to enhance the signal gain. The reflectivity of the two mirrors have a large impact on all properties of the amplifier, and must be chosen carefully in the VCSOA design. The reflectivity should be high enough to provide sufficient feedback so that high amplifier gain can be reached, but low enough so that lasing threshold cannot be reached when the single-pass gain is maximized. Too high mirror reflectivity results in low gain, narrow bandwidth, low saturation and high noise figure. The balance between the reflectivity of the mirrors and the gain provided by the active region is the central issue in VCSOA design. The vertical-cavity geometry gives VCSOAs a number of advantages over the in-plane design such as polarization independent gain and a circular-symmetric optical mode; the latter yields high coupling efficiency to optical fiber, which is instrumental in achieving a low noise figure.

Two generations of VCSOAs designed and fabricated at UCSB were presented. Both generations of devices were optically pumped and operated in reflection mode at 1.3-μm wavelength. The first generation was a planar structure with the goal of investigating basic VCSOA properties and develop theoretical models. The second generation used carrier confinement, which improved the efficiency of the devices as well as the maximum gain. The results are in summary 17 dB fiber-to-fiber gain, 6.1 dB noise figure, and -3.5 dBm saturation output power. Bandwidths between 20 and 100 GHz were measured.

Optical preamplification at 10 Gb/s was also presented in this paper. A VCSOA was operated at 11 dB fiber-to-fiber gain and a bandwidth of 37 GHz. The receiver sensitivity of a *PIN* receiver was improvement by a 7 dB resulting in a receiver sensitivity of –26.2 dBm. The narrow bandwidth of VCSOAs is a major advantage in this application as out-of-band noise is eliminated, making an additional optical filter redundant. Other potential applications include optical interconnects and switching and modulation. VCSOAs have the advantages of being compatible with low cost manufacturing techniques and fabrication of 2D arrays on wafer. The design also lends itself to monolithic integration with, for instance, VCSEL arrays or detector arrays. Tunable VCSOAs can be realized using the same technologies that have been used to make tunable VCSELs. The possibility of realizing arrays of very compact, low-cost devices, which could be tunable and/or integrated with other devices, makes VCSOAs a very promising technology for a wide range of applications in future optical communications systems.

ACKNOWLEDGEMENTS

REFERENCES

1.   F. Koyama, S. Kubota, K. Iga, "GaAlAs/GaAs active filter based on vertical cavity surface emitting laser", *Electron. Lett.,* **27**, pp. 1093-1095, 1991.
2.   R. Raj, J. A. Levenson, J. L. Oudar, M. Bensoussan, "Vertical microcavity optical amplifying switch," *Electron. Lett.,* **29**, pp. 167-169, 1993.
3.   R. Raj, J. L. Oudar, M. Bensoussan, "Vertical-cavity amplifying photonic switch," *Appl. Phys. Lett.*, **65**, pp. 2359-2361, 1994.
4.   N. Bouché, B. Corbett, R. Kuszelewicz, R. Ray, "Vertical-Cavity Amplifying Photonic Switch at 1.5 μm", *IEEE Photon. Technol. Lett.*, **8**, pp. 1035-1037, 1996.
5.   D. Wiedenmann, B. Moeller, R. Michalzik, K. J. Ebeling, "Performance characteristics of vertical-cavity semiconductor laser amplifers," *Electron. Lett.,* **32**, pp. 342-343, 1996.
6.   D. Wiedenmann, C. Jung, M. Grabherr, R. Jäger, U. Martin, R. Michalzik, K. J. Ebeling, "Oxide-confined vertical-cavity semiconductor optical amplifier for 980 nm wavelength", *CLEO 98 Tech. Dig.*, Paper CThM5, p. 378, 1998.
7.   R. Lewén, K. Streubel, A. Karlsson, S. Rapp, "Experimental Demonstration of a Multifunctional Long-Wavelength Vertical-Cavity Laser Amplifier-Detector", *IEEE Photon. Technol. Lett.*, **10**, pp. 1067-1069, 1998.
8.   E. S. Björlin, B. Riou, A. Keating, P. Abraham, Y.-J. Chiu, J. Piprek, J. E. Bowers, "1.3-μm Vertical-Cavity Amplifier," *IEEE Photon. Technol. Lett.*, **12**, pp. 951-953, 2000.
9.   E. S. Björlin, B. Riou, P. Abraham, J. Piprek, Y-J. Chiu, K. A. Black, A. Keating, J. E. Bowers, "Long Wavelength Vertical-Cavity Semiconductor Optical Amplifiers", *IEEE J. Quantum Electron.*, **37**, pp. 274-281, 2001.
10.   E. S. Björlin, J. E. Bowers, "Noise Figure of Vertical-Cavity Semiconductor Optical Amplifiers", *IEEE J. Quantum Electron.*, **38**, pp. 61-66, 2002.
11.   J. Piprek, S. Björlin, J. E. Bowers, "Design and Analysis of Vertical-Cavity Semiconductor Optical Amplifiers", *IEEE J. Quantum Electron.*, **37**, pp. 127-134, 2002.
12.   P. Royo, R. Koda, L. A. Coldren, "Vertical Cavity Semiconductor Optical Amplifiers: Comparison of Fabry-Perot and Rate Equation Approaches," *IEEE J. Quantum Electron.*, **38**, pp. 279-284, 2002.
13.   E. S. Björlin, J. Piprek, S. Gee, Y.-J. Chiu, J. E. Bowers, A. Dahl, P. Abraham, "1.3μm vertical-cavity amplifying switch," *OSA TOPS Optical Amplifier and Their Applictions*, **60**, pp. 154-160, 2001.
14.   E. S. Björlin, J. Geske, J. E. Bowers, "Optically preamplified receiver at 10 Gbit/s using vertical-cavity SOA," *Electron. Lett.,* **37**, pp. 1474-11475, 2001.

15. E. S. Björlin, P. Abraham, D. Pasquariello, J. Piprek, Y.-J. Chiu, J. E. Bowers, "High Gain, High Efficiency Vertical-Cavity Semiconductor Optical Amplifiers," *in Proc. 14th Indium Phosphide and Related Materials Conference,* pp. 307-310, 2002.

16. http://www.ece.ucsb.edu/Faculty/Coldren/UCSD.html

17. C. E. Zah, R. Bhat, B. N. Pathak, F. Favire, W. Lin, M. C. Wang, N. C. Andreadakis, D. M. Hwang, M. A. Koza, T. P. Lee, Z. Wang, D. Darby, D. Flanders, J. J. Hsieh "High-performance uncooled 1.3-μm AlxGayIn 1-x-yAs/InP strained-layer quantum-well lasers for subscriber loop applications", *IEEE J. Quantum Electron.*, **30**, pp. 511-523, 1994.

18. A. W. Jackson, R. L. Naone, M. J. Dalberth, J. Smith, K. J. Malone, D. W. Kisker, J. F. Klem, K. D. Choquette, D. Serkland, K. Geib, "OC-48 capable InGaAsN vertical cavity laser", *Electron. Lett.,* **37**, pp. 355-356, 2001.

19 S. Nakagawa, E. Hall, G. Almuneau, J. K. Kim, D. A. Buell, H. Kroemer, L. A. Coldren, "1.55-μm InP-Lattice-Matched VCSELs With AlGaAsSb-AlAsSb DBRs", *IEEE J. Select. Topics Quantum Electron.*, **7**, pp. 224-230, 2001.

20. V. Jayaraman, T. J. Goodnough, T. L. Beam, F. M. Ahedo, R. A. Maurice, "Continuous-wave operation of single-transverse-mode 1310-nm VCSELs up to 115 degrees C," *IEEE Photon. Technol. Lett.*, **12**, pp. 1595-1597, 2000.

21. D. Vakhshoori, J.-H. Zhou, M. Jiang, M. Azimi, K. McCallion, C.-C. Lu, K. J. Knopp, J. Cai, P. D. Wang, P. Tayebati, H. Zhu, P. Chen, "C-band tunable 6 mW vertical-cavity surface-emitting lasers", *OFC 2000 Tech. Dig. Postconf. Edition*, Paper PD13, pp. PD13-1-PD13-3, 2000.

22. http://www126.nortelnetworks.com/products/ml20_vcsel_tunable_laser.html

23. H. Ghafouri-Shiraz, *Fundamentals of laser diode amplifiers*, West Sussex, England: Wiley, 1996.

24. J. Piprek, E. S. Björlin, J. E. Bowers, "Optical gain-bandwidth product of vertical-cavity laser amplifiers," *Electron. Lett.,* **37**, p. 1, 2001.

25. T. Mukai, Y. Yamamoto, T. Kimura, "S/N and Error Rate Performance in AlGaAs Semiconductor Laser Amplifier and Linear Repeater Systems" *IEEE Trans. Microwave Theory Tech.*, **MTT-30**, pp. 1548-1556, 1982.

26. A. Black, A. R. Hawkins, N. M. Margalit, D. I. Babic, A. L. Jr. Holmes, Y.-L. Chang, P. Abraham, J. E. Bowers, E. L. Hu, "Wafer fusion: materials issues and device results", *IEEE J. Select. Topics Quantum Electron.*, **3**, pp. 943-951, 1997.

27. D. A. B. Miller, "Optical Interconnects to Silicon," *IEEE J. Select. Topics Quantum Electron.*, **6**, pp. 1312-1317, 2000.

28. C. Fan, B. Mansoorian, D. A. Van Blerkom, M. W. Hansen, V. H. Ozguz, S. C. Esener, G. C. Marsden, "Digital free-space optical interconnections: a comparison of transmitter technologies," *Appl. Opt.*, **34**, pp. 3103-3115, 1995.

29. P. Wen, M. Sanchez, O. Kibar, S. C. Esener, "Low-voltage, high contrast-ratio, low-noise VCSEL modulator," *in Proc. OSA Topical Mtg. on Optical Amplifiers and Their Applications*, pp. 265-266, 2000.

30. O. Kibar, P. J. Marchand, S. C. Esener, "Gain-bandwidth product of a VCSEL amplifier, " *LEOS 11th annual meeting*, pp. 221-222, 1998.

31. N. Suzuki, M. Ohashi, M. Nakamura, "A Proposed Vertical-Cavity Optical Repeater for Optical Inter-Board Connections", *Photon. Technol. Lett.*, **9**, pp. 1149-1151, 1997.

32. M. Ikeda, "Switching Characteristics of Laser Diode Switch", *IEEE J. Quantum Electron.*, **QE-19**, pp. 157-164, 1983.

33. M. Gustavsson, B. Lagerström, L. Thylén, M. Janson, L. Lundgren, A-C. Mörner, M. Rask, B. Stolz "Monolithically integrated 4 x 4 InGaAsP/InP laser amplifier gate switch arrays", *Electron Lett.*, **28**, pp. 2223-2225, 1992.

34. E. Almström, C. P. Larsen, L. Gillner, W. H. van Berlo, M. Gustavsson, E. Berglind, "Experimental and Analytical Evaluation of Packaged 4 x 4 InGaAsP/InP Semiconductor Optical Amplifier Gate Switch Matrices for Optical Networks", *IEEE J. Lightwave Technol.*, **14**, pp. 996-1004, 1996.

35. M. D. Feuer, J. M. Wiesenfeld, J. S. Perino, C. A. Burrus, G. Raybon, S. C. Shunk, N. K. Dutta, "Single-Port Laser-Amplifier Modulator for Local Access", *IEEE Photon. Technol. Lett.*, **8**, pp. 1175-1177, 1996.

36. N. Buldawoo, S. Mottet, F. Le Gall, D. Sigogne, D. Meichenin, S Chelles, "A semiconductor laser amplifier-reflector for the future FTTH applications", in *Proceedings of the 23rd European Conference on Optical Communication,* pp. 196-199, 1997.

37. H. Takesue, F. Yamamoto, T. Sugie, "Novel Node Configuration for DWDM Photonic Access Ring Using CMLS", *IEEE Photon. Technol. Lett.*, **12**, pp. 1698-1700, 2000.

38. E. S. Björlin, A. Dahl, J. Piprek, P. Abraham, Y.-J. Chiu, J. E. Bowers, "Vertical-Cavity Amplifying Modulator at 1.3-μm," *IEEE Photon. Technol. Lett.*, **13**, pp. 1271-1273, 2001.